Buckling and Postbuckling of Laminated Composite Plates with Ply Dropoffs

Marc T. DiNardo* and Paul A. Lagace†
Technology Laboratory for Advanced Composites,
Massachusetts Institute of Technology, Cambridge, Massachusetts

An experimental and analytical investigation was conducted on the buckling and postbuckling behavior of laminated graphite/epoxy plates with ply dropoffs under uniaxial compression. Three types of plates were considered: ply-dropoff plates with one or more internal plies terminated along a centerline perpendicular to the loading, flat plates to provide the baseline behavior, and angle-change plates where the fiber angle of several plies changes abruptly along the centerline. This latter case isolates the change in material properties without the geometric eccentricities present in ply-dropoff plates. An analysis method using a "superelement" formulated with a Rayleigh-Ritz assumed deflection model was developed and used to predict the linear buckling response of the plates. Both the experimental and analytical results show that ply dropoffs have a marked effect on plate buckling and postbuckling behavior. In contrast to basic flat plates, plates with ply dropoffs exhibit complex deflection shapes that cannot be characterized by simple modes. The buckling load of these plates was related to the ratio of the longitudinal bending stiffness of the dropped and undropped section of the plates and was bounded by the buckling loads of the flat plates with the layup configurations of the two individual sections. The angle-change plates exhibited much of the same behavior seen in the ply-dropoff plates but indicated that the change in the other bending stiffnesses also can have an important effect on the buckling behavior.

Nomenclature

a = plate length in x direction
A = in-plane area
$[A]$ = elastic stretching matrix
b = plate width in y direction
$[B]$ = elastic coupling matrix
$[D]$ = elastic bending matrix
$[D^*]$ = reduced bending stiffness matrix
N_x = applied load resultant in x direction
R_D = stiffness ratio
U = internal potential energy
w = deflection in z direction (out-of-plane)
$w_{,n}$ = slope tangent to normal
W = external work
x,y,z = plate coordinates
$\{\epsilon^0\}$ = strain vector at laminate midplane
$\{\kappa\}$ = curvature vector
Π_p = total potential energy

I. Introduction

AEROSPACE structural designers are increasingly making use of advanced composite materials to save weight and enhance structural performance. The orthotropic nature of these materials enables a structure to be efficiently tailored to meet given requirements. However, laminated materials require considerably more complex analyses than conventional materials as a result of their complex behavior. Consequently, these materials are only slowly coming into use in primary structures.

One technique used to optimize structural design is to taper the thickness of a component to match the specific load-carrying and stiffness requirements along the component. This is accomplished in metallic structures by machining (mechanically or chemically) the component. Since composite laminates are composed of plies with a fixed thickness, the best way to vary the thickness, and thus the stiffness and strength, of a composite structure is to terminate or "drop off" plies inside the laminate. Examples of such structures are the wing skin of the AV-8B aircraft,[1] where the skin thickness is varied from the root to the tip, and an interstage structure for the Ariane 4 launch vehicle, where a thin skin must be reinforced near a joint with an adjacent part.[2]

Some experimental[3] and analytical[4] work has been reported on the effects of ply dropoffs, but this has concentrated on the in-plane effects, particularly the local stress distribution around a ply dropoff. Since plates with ply dropoffs often are used in applications where compressive loads are important, and thus buckling is a primary concern, it is prudent to understand the effects of ply dropoffs in composite plates loaded in compression.

In most cases, plies are dropped off such that one side of a structure remains smooth. Thus, the presence of a ply dropoff results in both a change in elastic properties of the plate at the dropoff and an inherent eccentricity in the load path through the structure. The elastic couplings that are present in flat symmetric and unsymmetric plates also will affect the behavior of ply-dropoff plates and will lead to bending and twisting of a plate loaded inplane. All of these factors complicate the analysis and understanding of plates with ply dropoffs.

A large amount of work has been accomplished on composite plate buckling.[5] Most of this work, however, is restricted to symmetric laminated flat plates in which the elastic couplings are not as severe. Recently, some experimental and analytical work on unsymmetric composite plates with various inherent elastic couplings has been reported.[6,7] However, virtually no work is available on the buckling of plates with ply dropoffs,

Presented as Paper 87-0730 at the AIAA/ASME/AHS/ASEE 28th Structures, Structural Dynamics and Materials Conference, Monterey, CA, April 6-8, 1987; received Jan. 5, 1988; revision received Aug. 31, 1989.

*Currently Structural Design Engineer, General Electric Astro Space Division, Valley Forge, PA. Member AIAA.

†Associate Professor of Aeronautics and Astronautics. Member AIAA.

except for some very limited experimental observations.[1,2] The purpose of the current work is to provide a basic understanding of the behavior of composite plates with ply dropoffs.

II. Methodology

This study consists of both experimental and analytical efforts on the general buckling and postbuckling behavior of laminated plates with ply dropoffs. Because of the lack of information on such plates, a broad range of configurations was considered so that an initial understanding of the various effects resulting from ply dropoffs could be obtained. The study concentrated on the experimental work with a linear buckling analysis developed in support of the experimental work.

A. Experimental Program

Three types of plates were studied with a total of 17 laminate configurations and a total of 46 test specimens, as listed in Table 1, so that the various effects of the presence of ply dropoffs could be demonstrated and compared. All of the laminates were based on a $[\pm 45/0]_s$ configuration. The three types of plates considered are flat plates, plates with ply dropoffs, and plates with "angle changes," in the specimen configuration shown in Fig. 1. Several factors were varied in the layups considered: overall layup, the number of plies dropped off, the orientation of the dropped plies, and the arrangement of the dropped plies within the laminate.

All of the specimens have one flat side, since this is a typical configuration. This side serves as a flat, well-defined reference plane. Flat plates were used to determine the behavior of the layups of each section of ply-dropoff plates. In plates with ply dropoffs, the plies were always dropped off internally, since this is the most common method of terminating plies in structural applications. The plies were dropped off along the horizontal centerline of the specimen, as indicated in Fig. 1. A ply that is dropped off is notated by a subscript D.

In addition to the plates with ply dropoffs, plates were considered where the fiber orientation of a specific ply changed at the horizontal centerline. These angle-change plates were used to isolate the effect of the change in elastic properties at the dropoff line without the geometric eccentricities inherent in ply-dropoff plates. The notation $\theta_1 \rightarrow \theta_2$ indicates that the fiber angle of the ply is changed from θ_1 to θ_2 along the horizontal centerline of the plate.

Table 1 Test program

Laminate	Number of specimens	Plies dropped off, %	R_D
$[\pm 45/0]_s$	3	—	1
$[\pm 45/0_D/0/\mp 45]_T$	3	17	0.545
$[\pm 45/\bar{0}]_s$	1	—	1
$[\pm 45_2/0_2]_s$	4	—	1
$[\pm 45_2/0/0_D]_s$	4	17	0.545
$[\pm 45_2/0_{2D}/0_2/\mp 45_2]_T$	2	17	0.545
$[+45/+45_D/-45/-45_D/0/0_D]_s$	2	50	0.125
$[\pm 45_2/0]_s$	2	—	1
$[(\pm 45)_2/0_2]_s$	3	—	1
$[\pm 45/\pm 45_D/0_2]_s$	3	33	0.348
$[\pm 45/\pm 45_D/0/0_D]_s$	3	50	0.125
$[\pm 45/0]_{2s}$	4	—	1
$[\pm 45/0/(\pm 45/0)_D]_s$	3	50	0.098
$[\pm 45 \rightarrow 30/0]_{2s}$	3	—	[a]
$[\pm 45 \rightarrow 15/0]_{2s}$	2	—	[a]
$[\pm 30/0]_{2s}$	2	—	1
$[A^b/A_D/A]_T$	2	33	[a]

[a]Not applicable. [b]A indicates $[\pm 45/0]_s$ configuration.

B. Analytical Technique

Because of the discontinuous nature of plates with ply dropoffs, a Rayleigh-Ritz analysis with continuous modes over the entire plate could not be easily applied. Thus, the Rayleigh-Ritz method was used in conjunction with a finite-element aproach to develop a "superelement" to model the deflections over one-half of the plate. Two such elements were used to model the deflections over the entire plate.

The superelement is illustrated in Fig. 2. To model the specific configuration investigated herein, three sides of the element are clamped, and the fourth side is allowed to deform arbitrarily. This side corresponds to the ply-dropoff line and has four boundary nodes with both out-of-plane displacements and rotations as degrees of freedom. The eight interior nodes have only the out-of-plane displacement as degrees of freedom for a total of 16 degrees of freedom for the superelement. The boundary nodes are used to match conditions with the adjacent element along the ply-dropoff line.

Deflection modes are assumed and the total potential energy of the system is minimized to arrive at a solution. For general laminated composite plates, the internal potential energy is

$$U = \tfrac{1}{2}\iint_A \left[\{\epsilon^0\}^T[A]\{\epsilon^0\} + 2\{\epsilon^0\}[B]\{\kappa\} + \{\kappa\}^T[D]\{\kappa\}\right] dx\, dy \quad (1)$$

The bending-stretching coupling matrix exists because the midplanes of the two sections of the plate do not coincide. To

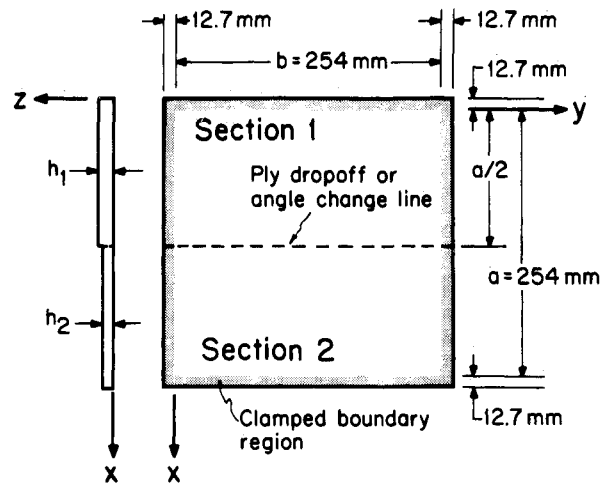

Fig. 1 Specimen configuration.

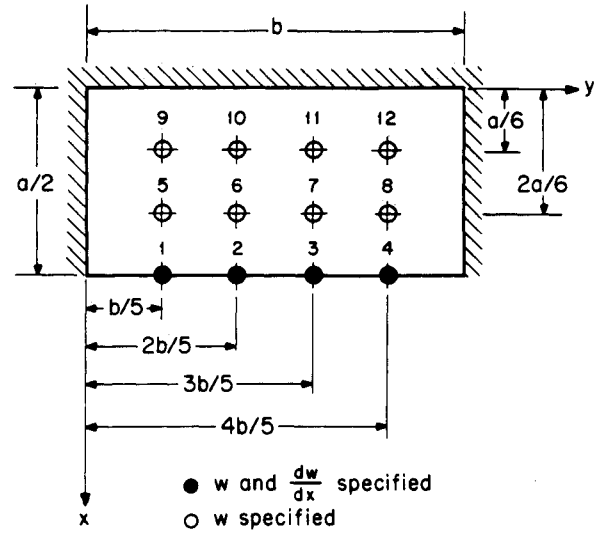

Fig. 2 Superelement geometry.

circumvent this complexity, a "reduced bending stiffness matrix"

$$[D^*] = [D] - [B]^T[A]^{-1}[B] \tag{2}$$

can be used[8] to decouple the equations into a more manageable form:

$$U = \iint_A \{\kappa\}^T[D^*]\{\kappa\}\, dx\, dy \tag{3}$$

The expression for Π_p

$$\Pi_p = U - W \tag{4}$$

is obtained by using the expression for the work done by the applied loading N_x of a thin plate in uniaxial compression:

$$W = -\frac{1}{2}\int\int_A N_x\left(\frac{dw}{dx}\right)^2 dx\, dy \tag{5}$$

In the Rayleigh-Ritz formulation, the accuracy of the solution is highly dependent on the assumed modes used to represent the deflections. It is assumed that the behavior can be adequately modeled by a finite series of separable functions for w. The assumed functions are standard beam vibration functions[9] that have been used successfully to predict the buckling and postbuckling behavior of symmetric and unsymmetric composite plates.[7]

The linear buckling problem is solved by using the principle of stationary minimum potential energy for the entire system. To match boundary conditions at the ply-dropoff line, the internal energy is expressed in terms of the deflections and slopes at the nodes of the superelement. A transformation matrix that relates the displacements and slopes to the modal displacement is developed and thus is used to match the boundary conditions along the ply-dropoff line for the two adjacent elements.

The solution results in a set of eigenvalues that yields the critical stress resultant at buckling and a corresponding set of eigenvectors. These eigenvectors are used with the aforementioned transformation matrix to determine the displacement field over the entire plate and generate isodeflection contour maps of the deflected surface, which can be compared with experimental results. Since the model is formulated in terms of the elastic properties of the two sections of the plate, the method can readily be used to analyze ply-dropoff, angle-change, and basic flat plates. The analysis was implemented in FORTRAN on a VAX 11/782 computer and is completely detailed in Ref. 10.

A hybrid stress finite-element analysis using a semi-Loof element[11,12] also was used to analyze the plates in this investigation to verify the effectiveness of the Rayleigh-Ritz method. The grid used in the finite-element analysis is shown in Fig. 3.

It should be noted that a full analysis of the behavior of the plates discussed herein requires a full nonlinear analysis, which was not attempted here. The purpose of the development of the linear analysis was to demonstrate the feasibility of the approach, provide a comparative prediction for the experimental results, and establish the basis for an efficient tool to analyze plates with ply dropoffs.

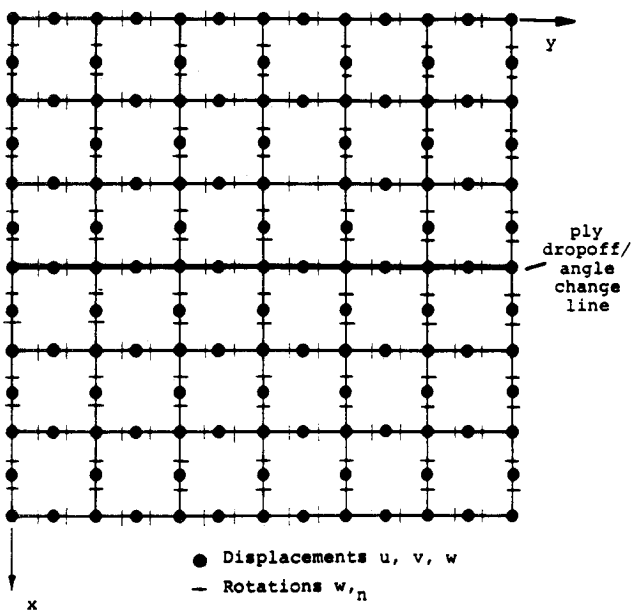

Fig. 3 Grid used in finite-element analysis.

III. Experimental Procedures

A total of 46 specimens were manufactured from Hercules AS4/3501-6 graphite/epoxy preimpregnated tape. The basic ply properties of this material are $E_L = 139.3$ GPa, $E_T = 11.1$ GPa, $G_{LT} = 4.9$ GPa, $\nu_{LT} = 0.3$, $t_{ply} = 0.134$ mm.

Standard procedures were used for the basic flat plates, but special techniques were necessary for proper fabrication of the ply-dropoff plates. A preliminary study indicated the need for accurate positioning of the dropped plies during the layup and careful smoothing of each ply to prevent the occurrence of voids along the ply-dropoff line. In cases where more than one ply was dropped off, the dropoffs were spaced apart by approximately 1.5 mm so that the top plies could readily conform to the underlying plies to reduce the likelihood of voids. For the plates with angle changes, the plies with angle changes were carefully cut and butted together so that the overall plate remained flat.

The laid-up plates were cured in an autoclave under 0.59 MPa pressure and 760 mm Hg vacuum with a 1-h hold at 116°C and a 2-h hold at 177°C. After an 8-h postcure at 177°C, the laminates were machined to the final dimensions of 279 mm square using a water-cooled diamond wheel. Each plate was instrumented with two pairs of back-to-back Micro-Measurements EA-060125 AC-350 strain gauges. For the flat plates, these gauges were located along the horizontal centerline, 12.7 mm off of the vertical centerline. For all of the other plates, these gauges were located 12.7 mm to the right of the vertical centerline and 25.4 mm above and below the horizontal centerline. In this manner, the strain behavior in each section of the plate near the dropoff/angle change line could be observed.

A modular loading jig, developed and verified in previous work,[6,7] was used with a 445-kN Material Test System (MTS) testing machine. All tests were done with clamped boundary conditions on all edges resulting in a square test section of 254 mm to a side. All plate edges were covered with Teflon tape to better allow inplane sliding at the edges but not allow out-of-plane deflections or slopes.

In addition to the strain, end-shortening, and load measurements taken, two types of out-of-plane deflection measurements were taken. In the first, a manually operated two-degree-of-freedom deflection tracker took data at points in a 9×9 grid while the plate was held at a constant load. The resulting data, referred to as a "scan," are used to generate isodeflection contour maps of the deflected shapes. In the second, a fixed array of nine displacement transducers in a 3×3 grid, shown in Fig. 4, was used to take continuous measurements of deflection load. Buckling loads were determined using the Southwell technique[13] and a linear regression program at three stations along the vertical centerline of the plate.

The actual testing began with an involved procedure to insure proper installation and alignment of the test specimen in the jig, which is fully described in Ref. 10. After alignment, each plate was loaded at a stroke rate of 0.42 mm/min until a point where the center plate deflection was one-half the thickness of the thinnest section of the plate. Previous work[6] has

shown that buckling has taken place before this point. At this point, a scan of the plate was taken. The plate then was loaded beyond this point, and the test was halted for a scan whenever an interesting mode shape developed. During loading, the nine displacement transducers recorded deflections. Loading continued until failure, which was defined as an abrupt drop in load of 30% or more.

IV. Results and Discussion

A. Initial Behavior

The onset of buckling, or significant out-of-plane deformation, was indicated by the divergence of the readings from the back-to-back strain gauges, as can be seen for a plate with a ply dropoff in Fig. 5. However, in almost all cases, particularly for the plates with ply dropoffs, out-of-plane deflection also was observed at low load, as opposed to true bifurcation buckling. Experimental buckling loads thus were calculated using the Southwell method, as previously indicated. These loads, as well as those predicted using the two analytical techniques, are presented in Table 2.

A number of observations can be made concerning the buckling loads of Table 2. In general, the analytical loads are fairly close to the experimentally measured loads, although the former are slightly higher as expected in the analysis of buckling. Furthermore, the present analysis gave nearly the same results as the more complicated hybrid stress finite-element analysis. The data are grouped in Table 2 such that the basic flat plates that correspond to the undropped and dropped sections of the ply-dropoff plates (sections 1 and 2, as noted in Fig. 1) are in the same group. This grouping makes it clear that the buckling

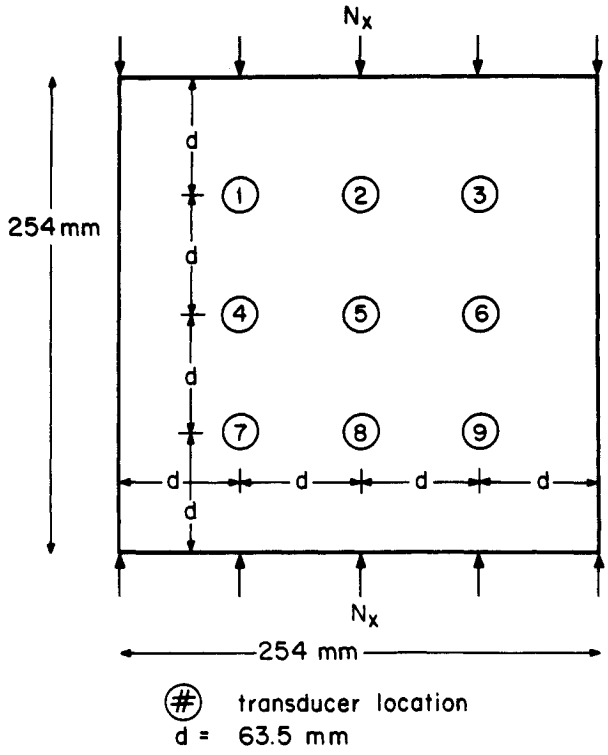

Fig. 4 Location of displacement transducers in fixed array.

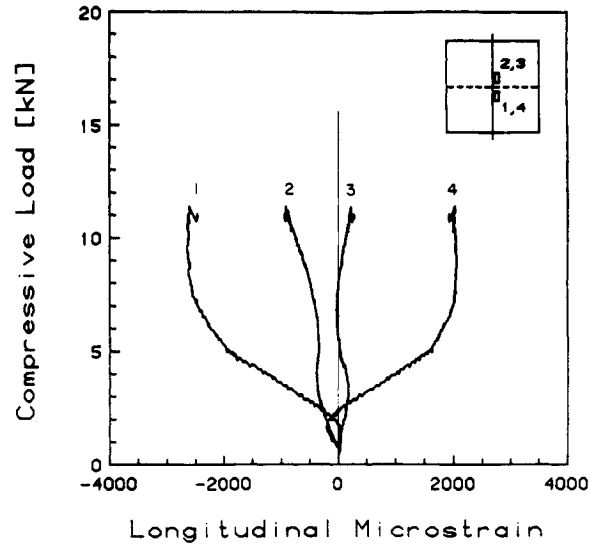

Fig. 5. Experimental plot of load vs surface strain showing divergence of gages indicating buckling.

Table 2 Measured and predicted buckling loads

	Buckling loads, kN		
		Predicted	
Laminate	Experimental	Method 1[a]	Method 2[b]
$[\pm 45/0]_S$	1.08(39%)[d]	1.04	0.96
$[\pm 45/0_D/0/\mp 45]_T$	1.05(31%)	0.15	0.14
$[\pm 45/\bar{0}]_S$	0.68(60%)	0.57	0.52
$[\pm 45_2/0_2]_S$	6.23(22%)	8.33	7.66
$[\pm 45_2/0/0_D]_S$	4.23(30%)	5.16	5.12
$[\pm 45_2/0_{2D}/0_2/\mp 45_2]_T$	3.13(15%)	5.16	5.12
$[+45/+45_D/-45/-45_D/0/0_D]_S$	2.04(7%)	1.71	1.67
$[\pm 45_2/0]_S$	3.33(12%)	4.57	4.19
$[(\pm 45)_2/0_2]_S$	5.99(19%)	8.74	8.08
$[\pm 45/\pm 45_D/0_2]_S$	2.70(17%)	3.46	3.55
$[\pm 45/\pm 45_D/0/0_D]_S$	1.83(11%)	1.76	1.67
$[\pm 45/0]_{2S}$	6.15(13%)	9.02	8.22
$[\pm 45/0/(\pm 45/0)_D]_S$	1.89(23%)	1.76	1.68
$[\pm 45 \rightarrow 30/0_2]_S$	4.90(39%)	9.02	8.18
$[\pm 45 \rightarrow 15/0_2]_{2S}$	3.76(22%)	8.94	8.04
$[\pm 30/0]_{2S}$	5.24(9%)	9.54	8.35
$[A^c/A_D/A]_T$	7.84(3%)	12.3	12.5

[a]Rayleigh-Ritz/superelement formulation. [b]Hybrid Stress finite element. [c]A indicates $[\pm 45/0]_S$ configuration. [d]Numbers in parentheses are coefficients of variation.

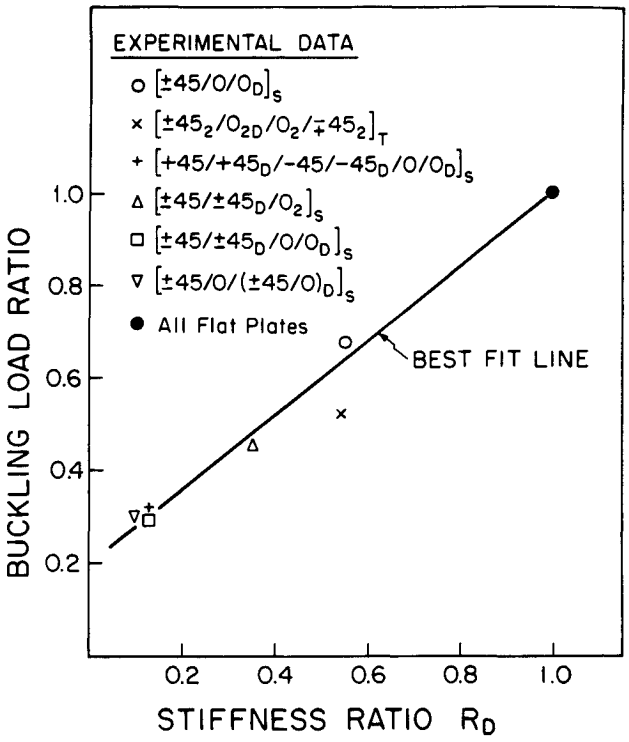

Fig. 6 Buckling loads of ply-dropoff plates normalized by buckling loads of undropped plates vs stiffness ratio.

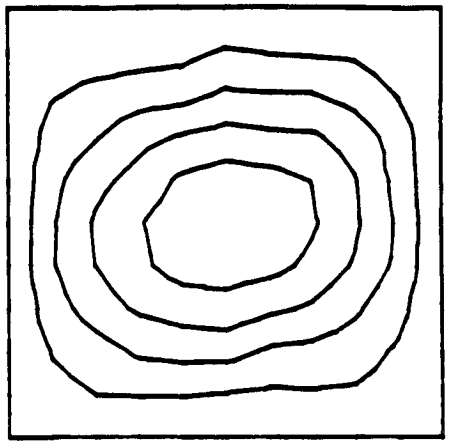

Fig. 7 Experimental isodeflection contour plot for $[\pm 45_2/0_2]_s$ plate.

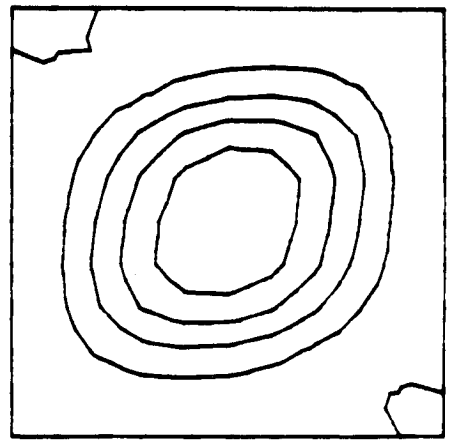

Fig. 8 Analytical isodeflections contour plot for $[\pm 45_2/0_2]_s$ plate.

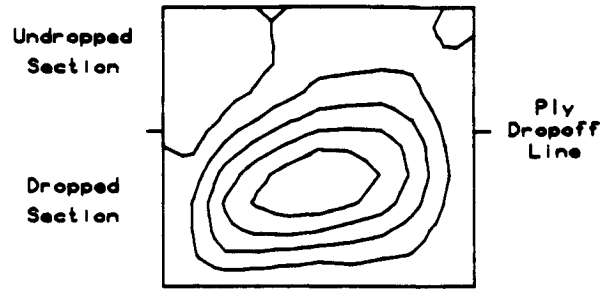

Fig. 9 Experimental isodeflection contour plot for $[\pm 45_2/0/0_D]_s$ plate.

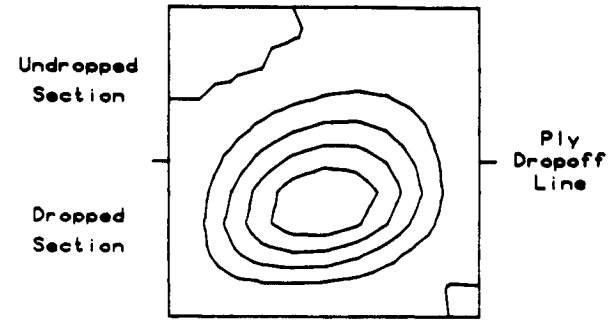

Fig. 10 Analytical isodeflection contour plot for $[\pm 45_2/0/0_D]_s$ plate.

load of the plates with ply dropoffs generally is bounded by the buckling loads of the two basic flat plates, which represent each of the sections of the ply-dropoff plate.

It also is apparent that the manner in which the plies are dropped off does affect the buckling load. This can be better quantified by examining the "stiffness ratio" of the plates, which is defined as the ratio of the longitudinal bending stiffness D_{11} of the dropped section of the plate to that of the undropped section (section 2 to section 1, as defined in Fig. 1). This ratio, denoted as R_D, is listed for all the plates in Table 1. Of course, flat plates have a ratio of 1, since the bending stiffness does not change along the plate. If the buckling loads of the ply-dropoff plates (excluding the 6-ply configuration) are normalized by the buckling loads of the corresponding basic plate with the undropped configuration and then are plotted against this stiffness ratio, a linear relationship is evident, as can be seen in Fig. 6. This also is true for the analytical results. Furthermore, plates with the same stiffness ratios have approximately the same reduction in buckling load independent of the manner in which plies are dropped off. This indicates that any effects due to the local eccentricity at the ply-dropoff line are overshadowed by the effects due to the stiffness difference between the two sections of the plate.

The buckling loads of the plates with angle changes were not bounded by the buckling loads of the flat plates representing the layup configuration of each of the individual sections for the one case with sufficient experimental data, $[\pm 45 - 30/0]_{2s}$. However, this may be attributable to the very high variation in the measured buckling loads for this particular plate. The two angle-change plates also do not follow the same trend as the ply-dropoff plates regarding the ratio of the buckling loads vs the stiffness ratio. In the basic flat-plate configuration, the buckling load increases as the fiber angle θ in the $[\pm\theta/0]_s$ laminate increases to 45 deg, although the longitudinal bending stiffness decreases. This occurs because the transverse bending stiffness D_{22} and the coupling terms D_{16} and D_{26} also play an important role in the buckling. In the plates where plies were dropped off, either the ratio of these three bending stiff-

nesses in the two sections of the plates was not significantly affected (when a 0-deg ply is dropped off) or is affected in approximately the same ratio as the longitudinal bending stiffness (when a +45 deg or −45 deg ply is dropped off). In the angle-change plates, the various bending stiffnesses are changed by differing ratios at the angle-change lines. This indicates that further effort is needed to understand better the contribution of the various bending stiffness terms in the buckling of these plates.

The presence of ply dropoffs or angle changes also considerably altered the buckling modes that the plates exhibited. The basic flat plates exhibited regular buckled deflection mode shapes, as can be seen in Fig. 7 for the $[\pm 45_2/0_2]_s$ laminate, as well as in the analytically predicted mode shape for this laminate shown in Fig. 8. The ply-dropoff and angle-change plates exhibited complex deflection shapes that could not be characterized by simple deflection modes. The degree of change from flat-plate behavior is related to the severity of the ply dropoff, in particular the R_D. The buckled shape of the plate with only two plies dropped off, $[(\pm 45)_2/0/0_D]_s$, exhibits movement of the point of maximum deflections away from the plate center, as shown in the experimentally measured isodeflection contours in Fig. 9 and those generated analytically in Fig. 10. A plate with a more severe ply dropoff of six plies, $[\pm 45/0/(\pm 45/0)_D]_s$, has the point of maximum deflection shifted to the center of the dropped section, as shown in Fig. 11, with almost all of the deflection occurring in the thinner half of the plate. Plates with similar R_D displayed similar deflection shapes. This again illustrates that the buckling behavior is controlled by this stiffness drop and not by the local eccentricity at the ply-dropoff line. Plates with angle changes exhibited shapes similar to plates with ply dropoffs, as can be seen for the $[\pm 45 - 15/0]_{2s}$ configuration in Fig. 12 (experimental) and Fig. 13 (predicted). However, since the stiffness changes were not as severe as in the cases where several plies are dropped off, the effects are not as dramatic as in these latter cases. Twisting also was observed in these isodeflection contours and is related to the bending-twisting coupling terms for the specific laminates.

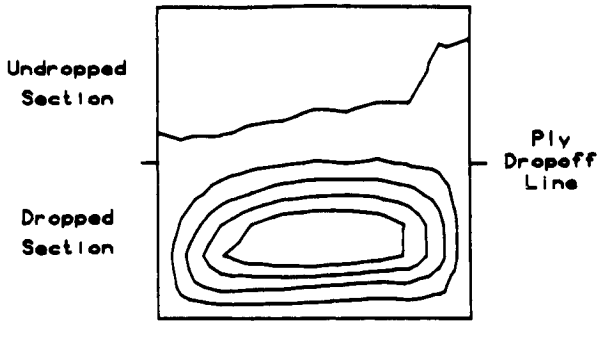

Fig. 11 Experimental isodeflection contour plot for $[\pm 45/0/(\pm 45/0)_D]_s$ plate.

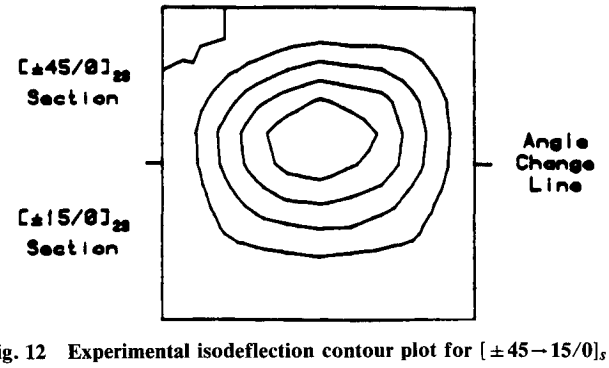

Fig. 12 Experimental isodeflection contour plot for $[\pm 45 - 15/0]_s$ plate.

B. Postbuckling Behavior

All of the plates showed considerable load-carrying capability beyond the buckling load. The majority of the plates transitioned into a higher-order bending shape at increased loads. This transition can be seen clearly in the load-deflection plot for the $[\pm 45/0]_{2s}$ laminate in Fig. 14, where the plate abruptly snaps into a completely different shape at approximately 9 kN.

The ply-dropoff plates again displayed markedly different load-deflection behavior, as can be seen in Fig. 15 for the $[\pm 45/0/(\pm 45/0)_D]_s$ plate with six plies dropped off. It is clear that the greatest deflections are in the thinner section of the plate (measurements 7–9). However, at higher loads the transition into a second shape is indicated by the readings at stations 1–6 switching from positive to negative at aproximately 2.5 kN and then increasing to a similar magnitude as those in the thinner part of the plate. In all cases, this transition was more gradual in the plates with ply dropoffs than in the basic flat plates. Some of the plates with angle changes did show a shape change, whereas others, such as the $[\pm 45 \rightarrow 15/0]_{2s}$ plate whose load-deflection behavior is shown in Fig. 16, did not.

All of the specimens failed along the boundaries generally at or near a corner and in the thinner section of the plates with ply dropoffs. Failure loads were generally over 10 times the buckling loads but are not considered to represent the true load-carrying capability of the plates, since they appear to be caused by the particulars of the test fixture and boundary conditions.

V. Summary

This work provides an important initial understanding of the buckling and postbuckling behavior of composite plates

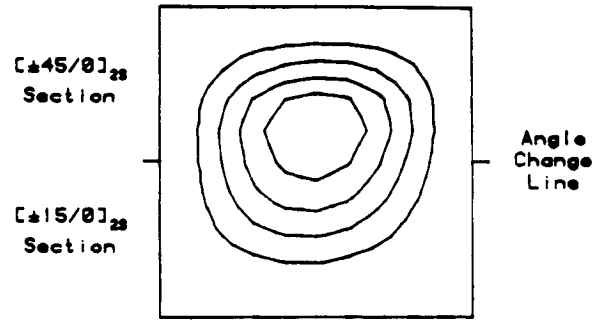

Fig. 13 Analytical isodeflection contour plot for $[\pm 45 - 15/0]_s$ plate.

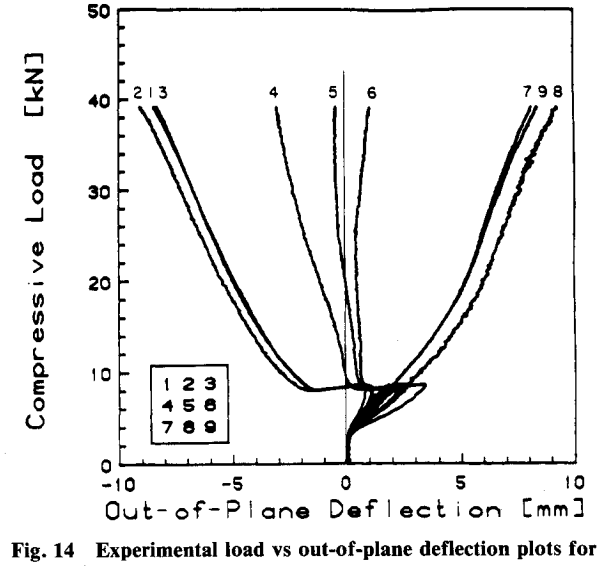

Fig. 14 Experimental load vs out-of-plane deflection plots for $[\pm 45/0]_{2s}$ plate.

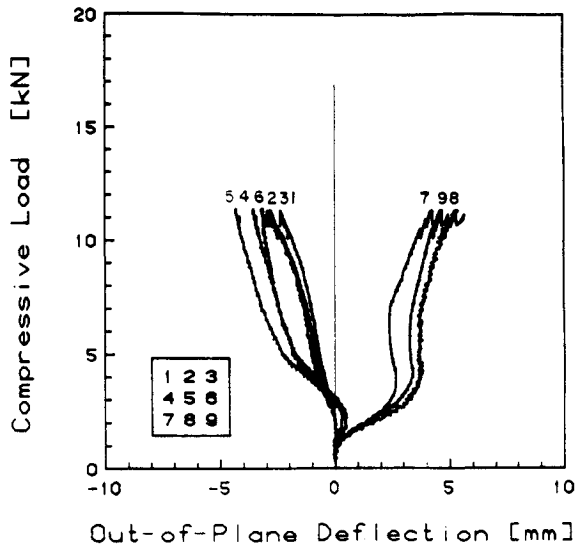

Fig. 15 Experimental load vs out-of-plane deflection plots for $[\pm 45/0/(\pm 45/0)_D]_S$ plate.

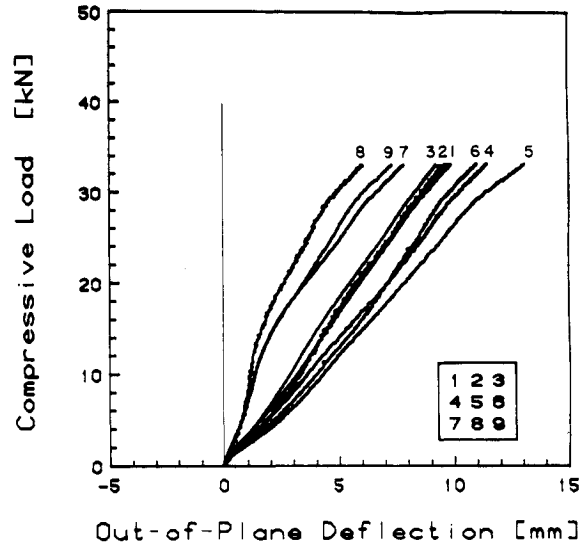

Fig. 16 Experimental load vs out-of-plane deflection plots for $[\pm 45-15/0]_{2S}$ plate.

with ply dropoffs and serves as the starting point for additional experimental and analytical work. Composite plates with ply dropoffs demonstrate more complex buckling and postbuckling behavior than basic plates, and the effects of these ply dropoffs depend on several factors. For the plates tested, the buckling load is bounded by the buckling loads of the basic flat plates with the same layup as the individual sections of the plate with the ply dropoffs. Furthermore, the reduction in the buckling load over the undropped section configuration is linearly related to the ratio of the longitudinal bending stiffnesses in the two sections of the plate. However, the results of the plates with angle changes indicate that this is particular to the ply-dropoff plates considered herein, since the transverse bending stiffness and coupling terms are affected in approximately the same manner in these ply-dropoff plates. The buckling loads of the plates with angle changes cannot be simply correlated with the longitudinal bending stiffness ratio as the various bending stiffnesses change by different ratios across the angle-change line. This indicates that further work should be conducted to understand the role of the various bending stiffnesses and their changes in plates with ply dropoffs on the buckling and postbuckling behavior. The results do strongly indicate that the local eccentricity due to the thickness change when plies are dropped off is insignificant compared with the effect of the bending stiffness changes. Furthermore, plates with ply dropoffs illustrate very complex deflection shapes.

The analysis method for the linear buckling load using a superelement for each section of the plates with ply dropoffs was very effective in predicting the buckling loads and was superior to the benchmark finite-element method used in terms of giving similar results in less than one-tenth the computer time. However, bifurcation buckling generally was not observed in the tests; thus the analysis method needs to be extended to the nonlinear regime for full postbuckling analysis. The concept of the superelement serves as a basis for this nonlinear analysis, and additional elements could be readily developed to allow for multiple dropoff lines and different boundary conditions.

Acknowledgments

Support for this work was provided by the Boeing Military Airplane Company under Contract BMAC P.O. AA0045. The authors wish to acknowledge the invaluable assistance of Professor John Dugundji of the Massachusetts Institute of Technology's Department of Aeronautics and Astronautics in formulating the analytical technique presented herein.

References

[1]Potter, R. T., "The Significance of Defects and Damage in Composite Structures," *AGARD Conference on Characterization, Analysis, and Significance of Defects in Composite Materials,* AGARD-CP-355, 1983.

[2]Blass, C. and Wiggenrad, F.F.M., "Development and Test Verification of the Ariane 4 Interstage 2/3 in CFRP," *Proceedings of the AIAA/ASME/ASCE/AHS 27th Structures, Structural Dynamics, and Materials Conference,* AIAA, New York, May 1986, pp. 307-313.

[3]Grimes, G. C. and Dusablon, E. G., "Study of Compressive Properties of Graphite/Epoxy Composites with Discontinuities," *Composite Materials: Testing and Design, ASTM STP 787,* American Society for Testing and Materials, Philadelphia, PA, 1982, pp. 513-538.

[4]Kemp, B. L. and Johnson, E. R., "Response and Failure Analysis of a Graphite-Epoxy Laminate Containing Terminating Internal Plies," *Proceedings of the AIAA/ASME/ASCE/AHS 26th Structures, Structural Dynamics, and Materials Conference,* AIAA, New York, April 1985, pp. 13-24.

[5]Leissa, A. W., "Buckling of Laminated Composite Plates and Shell Panels," Air Force Wright Aeronautical Laboratories, Wright-Patterson AFB, OH, AFWAL-TR-85-3069, June 1985.

[6]Lagace, P. A., Jensen, D. W., and Finch, D. C., "Buckling of Unsymmetric Composites," *Composite Structures,* Vol. 5, No. 2, 1986, pp. 101-123.

[7]Jensen, D. W. and Lagace, P. A., "Influence of Mechanical Couplings on the Buckling and Postbuckling Behavior of Anisotropic Plates," *AIAA Journal,* Vol. 26, October 1988, pp. 1269-1277.

[8]Ashton, J. E., "Approximate Solutions for Unsymmetric Laminated Plates," *Journal of Composite Materials,* Vol. 3, Jan. 1969, pp. 189-191.

[9]Young, D., "Vibrations of Rectangular Plates by the Ritz Method," *Journal of Applied Mechanics,* Vol. 17, Dec. 1950, pp. 448-453.

[10]DiNardo, M. T., "Buckling and Postbuckling of Laminated Composite Plates with Ply Dropoffs," Massachusetts Institute of Technology, Cambridge, MA, TELAC Rept. 86-13, May 1986.

[11]Pian, T. H. H., "Finite Elements Based on Consistently Assumed Stresses and Displacements," *Finite Elements in Analysis and Design,* Vol. 1, April 1985, pp. 131-140.

[12]Wang, C., Pian, T. H. H., Dugundji, J., and Lagace, P. A., "Analytical and Experimental Studies on the Buckling of Laminated Thin-Walled Structures," *Proceedings of the AIAA/ASME/ASCE/AHS 28th Structures, Structural Dynamics and Materials Conference,* AIAA, New York, April 1987, pp. 135-140.

[13]Southwell, R. V., "On the Analysis of Experimental Observations in Problems of Elastic Stability," *Proceedings of the Royal Society of London, Ser. 1,* Vol. 135, 1932, pp. 601-616.